Stable long-range interhemispheric coordination is supported by direct anatomical projections

Kelly Shen[a,1,2], Bratislav Mišić[b,1], Ben N. Cipollini[c], Gleb Bezgin[a], Martin Buschkuehl[d], R. Matthew Hutchison[e], Susanne M. Jaeggi[f], Ethan Kross[g], Scott J. Peltier[h], Stefan Everling[i,j], John Jonides[g], Anthony R. McIntosh[a,k], and Marc G. Berman[l,m]

[a]Rotman Research Institute, Toronto, ON, M6A 2E1, Canada; [b]Department of Psychological and Brain Sciences, Indiana University, Bloomington, IN 47405; [c]Department of Computer Science and Engineering, University of California, San Diego, La Jolla, CA 92093; [d]MIND Research Institute, Irvine, CA 92617; [e]Center for Brain Science, Harvard University, Cambridge, MA 02138; [f]School of Education and Department of Cognitive Science, University of California, Irvine, CA 92697; [g]Department of Psychology and [h]Functional MRI Laboratory, University of Michigan, Ann Arbor, MI 48109; [i]Department of Physiology and Pharmacology and [j]Robarts Research Institute, University of Western Ontario, London, ON, N6A 5K8, Canada; [k]Department of Psychology, University of Toronto, Toronto, ON, M5S 3G3, Canada; and [l]Department of Psychology and [m]Grossman Institute for Neuroscience, Quantitative Biology and Human Behavior, University of Chicago, Chicago IL 60637

Edited by Michael S. Gazzaniga, University of California, Santa Barbara, CA, and approved April 14, 2015 (received for review February 18, 2015)

The functional interaction between the brain's two hemispheres includes a unique set of connections between corresponding regions in opposite hemispheres (i.e., homotopic regions) that are consistently reported to be exceptionally strong compared with other interhemispheric (i.e., heterotopic) connections. The strength of homotopic functional connectivity (FC) is thought to be mediated by the regions' shared functional roles and their structural connectivity. Recently, homotopic FC was reported to be stable over time despite the presence of dynamic FC across both intrahemispheric and heterotopic connections. Here we build on this work by considering whether homotopic FC is also stable across conditions. We additionally test the hypothesis that strong and stable homotopic FC is supported by the underlying structural connectivity. Consistent with previous findings, interhemispheric FC between homotopic regions were significantly stronger in both humans and macaques. Across conditions, homotopic FC was most resistant to change and therefore was more stable than heterotopic or intrahemispheric connections. Across time, homotopic FC had significantly greater temporal stability than other types of connections. Temporal stability of homotopic FC was facilitated by direct anatomical projections. Importantly, temporal stability varied with the change in conductive properties of callosal axons along the anterior–posterior axis. Taken together, these findings suggest a notable role for the corpus callosum in maintaining stable functional communication between hemispheres.

functional connectivity | structural connectivity | homotopy | dynamics

The brain's capacity for processing information relies on a modular and hierarchical functional architecture that allows both functional segregation and integration (1, 2). Distributed processing occurs within segregated communities responsible for highly specialized functions, whereas more comprehensive functions require long-range integration across communities. This long-range integration is especially important for coordinating functions between the two hemispheres. Functional connectivity (FC), computed as the temporal correlation or covariance between regionwise signals, varies across different interhemispheric regions. FC is significantly stronger between homotopic regions than between heterotopic regions (3) and is greater than would be expected from the anatomical distance between the homotopic regions (4). This strong homotopic FC is thought to be mediated by the strong underlying structural connectivity of the corpus callosum (CC). Indeed, the majority of callosal fibers are between homotopic brain regions (5–7), and the loss of callosal integrity leads to a loss in homotopic FC (8, 9).

Recently, a growing number of resting-state functional MRI (fMRI) studies have reported how FC varies over time (10). Flexibility in cognitive processing is thought to arise from the ability of certain regions to participate dynamically in different network configurations (11). For instance, interhemispheric functional interactions between different communities are highly variable over the course of a resting-state scan. Meanwhile, interhemispheric connections within the same community, especially homotopic connections, are temporally stable (12–14). Together, these findings suggest that interhemispheric coordination may occur predominantly via homotopic functional connections.

FC also is known to vary between task and resting-state conditions (15). The extent to which interhemispheric coordination relies on homotopic functional connections across conditions remains to be determined. Moreover, whether interhemispheric coordination is mediated by the underlying structural connectivity has yet to be demonstrated empirically. In this study, we tested the hypothesis that FC between homotopic regions is stable across both time and conditions using blood oxygen level-dependent (BOLD) fMRI data collected from humans and macaques. We additionally used two approaches to examine the extent to which the stability of homotopic functional connections is mediated by the underlying anatomical projections. First, we directly compared macaque BOLD-fMRI data with structural connectivity data derived from axonal tract-tracing studies in macaque monkeys. Second, we compared the patterns of observed functional stability with known patterns of callosal fiber conductive properties in both humans and macaques.

Significance

We show that the functional coordination between the two hemispheres of the brain is maintained by strong and stable interactions of a specific subset of connections between homotopic regions. Our data suggest that the stability of those functional interactions is mediated in part by the direct anatomical projections of large, highly myelinated fibers that traverse the corpus callosum. These functional properties were evident in both humans and macaques, suggesting a preserved framework for interhemispheric communication despite an increase in functional lateralization in humans. These results contribute to our fundamental understanding of how dynamic functional interactions between the two hemispheres of the mammalian brain are supported by its underlying anatomical architecture.

Author contributions: K.S., B.M., S.E., J.J., A.R.M., and M.G.B. designed research; B.N.C., G.B., M.B., R.M.H., S.M.J., E.K., and S.J.P. performed research; K.S., B.M., B.N.C., and M.G.B. analyzed data; and K.S., B.M., and M.G.B. wrote the paper.

The authors declare no conflict of interest.

This article is a PNAS Direct Submission.

[1]K.S. and B.M. contributed equally to this work.

[2]To whom correspondence should be addressed. Email: kshen@research.baycrest.org.

This article contains supporting information online at www.pnas.org/lookup/suppl/doi:10.1073/pnas.1503436112/-/DCSupplemental.

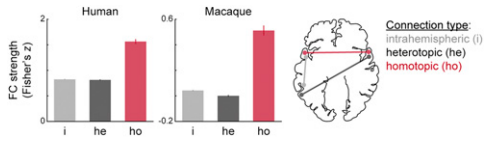

Fig. 1. Mean (± SEM) FC strength for intrahemispheric (i), heterotopic (he), and homotopic (ho) connections in humans and macaques.

Results

fMRI data from one human and one macaque study were included for analysis. In the human study, each participant underwent a series of four scans in the same experimental session. The first, second, and fourth scans were unconstrained resting-state conditions (RS1–3); during the third scan participants were instructed to think about a negative autobiographical memory ('induced rumination"; IR), which increased subjective feelings of negative mood (16). In the macaque study, each animal underwent two consecutive resting-state scans under light anesthesia (17). For both studies, FC was calculated as regionwise Pearson correlations of BOLD time series. Functional connections were stratified into homotopic (interhemispheric connections between homologous regions), heterotopic (interhemispheric connections between nonhomologous regions), and intrahemispheric connections. Because the parcellations for both datasets were symmetric, this categorization was made on the basis of the anatomical labels of each region of interest (ROI) rather than on symmetry in coordinate space.

Consistent with previous findings (4, 18), homotopic connections were significantly stronger on average than either heterotopic or intrahemispheric connections in both humans (Kruskal–Wallis, $P < 0.001$) and monkeys ($P < 0.001$) (Fig. 1). A post hoc analysis revealed that the FC strength of all three types of connections in both datasets were significantly different from one another (Tukey–Kramer method for multiple comparisons, all adjusted $P < 0.05$), with homotopic being the strongest followed by intrahemispheric and then heterotopic connections. The difference in strength between intrahemispheric and heterotopic connections was more pronounced in macaques than in humans (mean difference: 0.042 vs. 0.010, respectively).

Stability Across Conditions. To investigate the stability of functional connections across conditions, a multivariate partial least squares (PLS) (19) analysis was performed to isolate a pattern of FC that robustly differentiated experimental conditions (Fig. 2*A*). PLS produces an index ("salience") for each connection that represents the extent to which that connection changes between conditions. For the human dataset, the PLS analysis resulted in a significant latent variable (LV) ($P = 0.02$, cross-block covariance = 72%). This LV's design contrast differentiated the IR condition from RS3 (Fig. 2*B*, *Left*). Interestingly, homotopic connections had significantly smaller saliences than the other types of connections (Tukey–Kramer, adjusted $P < 0.05$) (Fig. 2*B*, *Right*), suggesting that they were the least variable across conditions. There was no difference in condition variability between intrahemispheric and heterotopic connections (adjusted $P > 0.05$). These results seemed to be driven mostly by the contrast between the IR and RS3 conditions, and limiting the PLS analysis to only these conditions produced similar results (*SI Results*). These results suggest that homotopic FC, in addition to being significantly stronger, is significantly more stable across resting-state and IR conditions.

A PLS analysis of the macaque dataset resulted in a contrast that differentiated the two resting-state conditions (Fig. 2*C*, *Left*). Again, homotopic connections had smaller saliences than the other types of connections, but this effect did not reach significance (LV: $P = 0.63$; Kruskal–Wallis, $P = 0.29$) (Fig. 2*C*, *Right*). Accordingly, we did not consider the stability of FC across conditions in the macaque dataset in subsequent analyses.

Stability Across Time. To examine the stability of functional connections across time, we first determined how FC changed over the course of each scan by computing regionwise Pearson correlations using a sliding-window approach. We then computed the autocorrelation coefficient of each functional connection over time (Fig. 3*A*). In this analysis, a larger coefficient indicates a more consistent functional connection over the course of the scan. In all conditions, for both datasets, homotopic connections were significantly more stable across time than other types of connections for a window size of 60 s (Tukey–Kramer method, adjusted $P < 0.05$) (Fig. 3*B*). Because the data were similar across conditions, we collapsed the temporal stability measures across conditions for subsequent analyses. Results for other window sizes (30 s and 120 s) were similar (Fig. S1). Together with our findings of stable homotopic FC across multiple resting-state and IR scans, these results indicate that homotopic functional connections are highly consistent over time.

Functional Stability, Distance, and Anatomical Connectivity. The strength of homotopic FC has been shown to be greater than would be expected from the distance between regions (4). Using the same datasets, we previously have reported how changes in FC across conditions are independent of the spatial distance between regions (20) and how FC changes across time are only weakly related to distance (14). Of relevance here, homotopic connections were exceptionally stable across time and conditions despite spanning a range of distances (*SI Results*, Figs. S2 and S3, and Table S1). These data suggest that functional stability is independent of distance and instead may be mediated by the underlying white matter connectivity.

We examined the extent to which structural connectivity influenced homotopic stability by analyzing the relationship between structural connectivity (derived from axonal tract-tracing studies in macaques) and our finding of high homotopic temporal stability in macaques. Homotopic regions that were not directly structurally connected were the right and left retrosplenial cingulate cortex, subgenual cingulate cortex, gustatory cortex, hippocampus, anterior insula, dorsomedial prefrontal cortex, orbitolateral prefrontal cortex, and primary visual cortex (21–24). We performed a two-way ANOVA between temporal stability, hemispheric classification (intrahemispheric, heterotopic, and homotopic), and structural connectivity. It revealed a significant main effect of structural connectivity as a function of FC stability ($P < 0.001$) (Fig. 4*A*) as well as a significant main effect of hemispheric classification ($P < 0.001$) for data constructed using a 60-s sliding window. The interaction of structural connectivity and hemispheric classification also was significant ($P < 0.05$), and a post hoc Bonferroni analysis showed that the structurally connected homotopic pairs were significantly more stable in their dynamic FC than all other types of pairs (adjusted $P < 0.05$). Homotopic pairs without direct structural connectivity were no different in their temporal stability than heterotopic or intrahemispheric pairs (adjusted $P > 0.05$). Intrahemispheric pairs also differed significantly in their FC stability as a function of structural connectivity so that regions that had direct anatomical connections were more stable (adjusted $P < 0.05$). However, the temporal stability of heterotopic pairs did not vary with structural connectivity (adjusted $P > 0.05$). These results were not idiosyncratic to the choice of window size, because similar patterns were observed when temporal stability was computed using other window sizes (Fig. S4). There were a few notable exceptions to temporal stability in homotopic pairs lacking direct structural connectivity. The homotopic interactions of gustatory (G), primary visual (V1), and, to a lesser extent, retrosplenial cingulate (CCr) cortices were >1 SD above the mean temporal stability for homotopic pairs lacking direct structural connectivity and were nearly as stable as those between homotopic pairs that had direct structural connectivity (Fig. 4*A* and Fig. S4, filled circles).

The axonal composition of the macaque CC is known to vary along the anterior–posterior (A–P) axis and follows a hierarchical organization (Fig. 4*B*) (25–27). The anterior portion of the

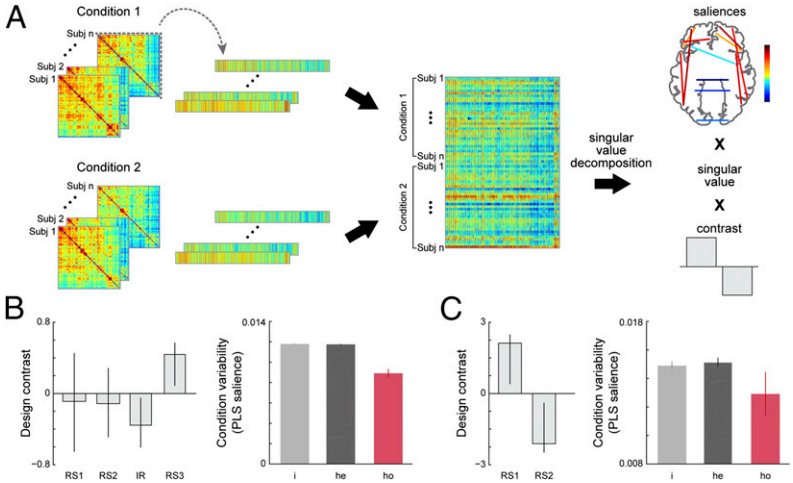

Fig. 2. Variability of FC across conditions. (*A*) Schematic for PLS analysis. FC matrices were created for each condition in each subject, and then vectorized by taking their upper triangles. These FC vectors were stacked to create a data matrix ordered by subject and then by condition. The covariance between FC and the experimental conditions was computed, and a singular value decomposition was performed on the covariance matrix. The resulting LV includes a contrast between conditions, a scalar singular value, and a set of saliences (depicted as weighted connections) that describe the extent to which each functional connection changes across conditions. (*B* and *C*) Design contrast (± 95% confidence interval) and condition variability (mean ± SEM) for intrahemispheric (i), heterotopic (he), and homotopic (ho) connections in humans (*B*) and macaques (*C*).

callosum has higher axon density, lower percentage of myelination, and smaller axon diameters. These axons serve the prefrontal polysensory association areas. Axon density then decreases with a concomitant increase in myelination and axon diameter toward the posterior of the CC. These axons serve the somatosensory, motor, and posterior parietal cortices. Finally, axon density increases again and is accompanied by a decrease in axon diameter at the most posterior end of the CC, whereas the percentage of myelination seems to plateau. These axons serve the inferior temporal and visual cortices. The morphological features of the CC therefore suggest that its conductive properties vary along the A–P axis and may influence the functional characteristics of interhemispheric communication. Fig. 4*C* shows how the temporal stability of homotopic functional connections with direct structural connectivity follows the A–P pattern of the CC for macaque data computed using a 60-s window, with correlations between the patterns of temporal stability and conduction properties of the CC being both strong and significant (Table S2). Results from other window sizes were similar (Fig. S4). The axonal density of the human CC follows a pattern similar to that of the macaque (Fig. 4*D*) (28). The temporal stability of homotopic functional connections in humans computed using a 60-s window also was similar to that observed in macaques (Fig. 4*E*). This pattern of temporal stability in humans was negatively correlated with overall axonal density (fiber diameters >0.4 μm; $r = -0.69$, $P < 0.05$) and positively correlated with the density of the largest diameter axons in the callosum (fiber diameters >5 μm; $r = 0.68$, $P < 0.05$; also see *SI Results*, Fig. S5, and Table S3). Together, these data suggest that both the presence of an underlying anatomical projection and the conduction-related characteristics of the white matter fiber tracts are important for mediating homotopic stability. Thus direct structural connectivity is a crucial determinant of the dynamics of homotopic functional interactions.

Discussion

Our results highlight the unique contribution of homotopic connections to global communication. We found that homotopic connections were stable across multiple resting-state and IR scans as well as across time. High stability of homotopic connections was independent of distance and instead was supported primarily by direct axonal projections following a pattern consistent with the characteristics of the CC. These data suggest that homotopy is an anatomical design principle that serves to anchor functional interactions between the hemispheres, presumably allowing information to become integrated in a reliable way.

Several recent studies have demonstrated a causal role for the CC in interhemispheric FC: Severing of callosal projections reduces interhemispheric FC (8, 9, 29–31, but see ref. 32), whereas the anterior commissure may be a prominent noncallosal conduit for interhemispheric coordination (29, 33, 34). For instance, O'Reilly et al. (29) found that interhemispheric FC could be largely preserved following complete section of the CC, as long as the anterior commissure was left intact. We add to these findings by showing how direct structural projections contribute not only to the magnitude of homotopic functional connections but also to their stability. Moreover, we show how functional stability varies with the change in conduction properties of the CC along the A–P axis.

The strength of resting-state FC is known to decrease with increasing distance (e.g., ref. 35). For intrahemispheric FC, this distance effect may partially result from the decrease in intrahemispheric structural connectivity with increasing distance (36). However, the strength of homotopic FC is known to be independent of the distance between regions (4). Our observations that the high functional stability between homotopic regions across both time and conditions could not be accounted for by distance complement these previous findings (also see refs. 14 and 20). Together, these data suggest that the structural connectivity between homotopic regions may not follow the same distance-dependent relationship as that reported for intrahemispheric structural connectivity. Instead, the strong coherence between homotopic areas may arise from specific properties of white matter projections traversing the CC. Previous cytological studies report that the pattern of myelination of the callosum follows a hierarchical organization. The primary sensory cortices are connected by the largest myelinated axons and relatively few unmyelinated axons, whereas the opposite is true of association areas, which tend to be connected by some small myelinated axons and relatively many unmyelinated axons (25–28). Our data show how the stability of functional interactions between homotopic areas follows a similar pattern (also see ref. 37). The inverse correlations we observed in humans between axon density and homotopic stability for thin and thick fibers (Table S3) were likely driven by the same underlying volumetric constraints of the callosum, whereby a trade-off exists between having many thin fibers or fewer thick fibers (38, 39). Together with the evidence that most axons of the callosum serve homotopic connections (5–7), our findings lend further support to the notion that homotopic

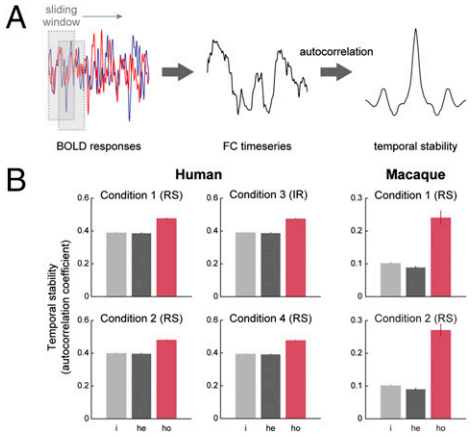

Fig. 3. Stability of FC across time. (*A*) Schematic for temporal stability analysis. FC was computed using a sliding-window approach to produce an FC time series for each connection. Each FC time series was cross-correlated with itself to produce a normalized autocorrelation coefficient. The average autocorrelation coefficient across all lags was used as a temporal stability metric. (*B*) Temporal stability (mean ± SEM) in all task conditions for intrahemispheric (i), heterotopic (he), and homotopic (ho) connections in humans (*Left*) and macaques (*Right*) from data computed using a 60-s sliding window. See Fig. S1 for other window sizes.

functional connectivity is conditioned on the hierarchical organization of anatomical brain networks.

Several other possible mechanisms for strong homotopic communication have been posited and also may contribute to the consistency in FC that we observed across time and conditions. First, much of homotopic coherence may be a result of indirect (i.e., polysynaptic) projections (29, 32). These may include subcortical structures such as thalamus and the basal forebrain (7). For instance, macaque primary visual cortices exhibit strong homotopic FC (33) despite limited callosal projections (24, 40). Similar observations have been reported in humans (41–43). In the current study, we additionally observed very stable homotopic connectivity in macaque V1. These observations of V1 coherence may arise from the common input provided by the lateral geniculate nucleus (44). Second, the modulatory effects of ascending arousal systems (45) may be symmetric, potentially contributing to coherent low-frequency fluctuations in homotopic brain areas (4). Interestingly, a recent study has reported how the basal forebrain accounts for at least some of the temporal dynamics of resting-state FC (46).

The possibility that physiological characteristics of anatomical connections between homotopic brain areas may serve to establish stable functional connections between those areas raises the question: What is the significance of these structural and functional relationships in the context of global network organization and communication? A recent study has shown how the strongest functional correlations within V1 exist between neurons that have similar receptive fields, especially between those having bidirectional anatomical connectivity (47). Although relatively few in number, the strongest functional connections were associated with a disproportionately large portion of the total synaptic weight, suggesting that synaptic computations may be driven by just a few inputs that share a functional role, whereas most other inputs are only modulatory (48). Extrapolating these findings to the level of large populations of neurons that form regions serving distinct functions, one could speculate that most of the structural connections between homotopic regions act as drivers, with homotopic projections making disproportionate contact with neurons that share a functional role. Thus structural connections between heterotopic regions may act predominantly as modulators connecting neurons across regions that do not necessarily share a functional role. It stands to reason that as information processing becomes less restricted to information received via receptive fields—as it does going from unimodal to heteromodal processing regions—the proportion of driving to modulatory inputs could decrease. This decrease would be in line with the observations that the strength (18) and stability of functional connections decreases with processing hierarchy. Further studies are needed to test this hypothesis directly. Nevertheless, the significance of homotopic connections for network communication is clearly emerging. Recent simulation studies have shown that functional networks are best modeled when homotopic structural connections are present (49, 50). In contrast, the addition of heterotopic structural connections resulted in less accurate simulations, suggesting that heterotopic connections play a significantly smaller role in interhemispheric coordination (50). The structural connectivity provided by both the CC and the anterior commissure has been shown to decrease proportionally with the evolutionary expansion in brain size, whereas intrahemispheric structural connectivity has increased (51). This pattern suggests that the two hemispheres of the brain have become increasingly independent and possibly contributes to the functional lateralization observed in humans (27, 52). However, functional lateralization in humans also may arise from an increase in conduction delays resulting from larger brain sizes (53). Our data suggest that despite the evolutionary increase in intrahemispheric structural connectivity, interhemispheric functional coordination in the human brain remains exceptionally strong and stable and may be the result of the underlying structural connections (also see ref. 54). This notion is consistent with observations that the thickest callosal fibers, those serving primary and unimodal areas, scale with brain size across species, but the thinnest ones, those serving association areas, do not (55). Moreover, a recent clinical study found that homotopic functional connections are disrupted across a wide range of psychiatric conditions, including attention deficit hyperactivity disorder, major depression, and schizophrenia (56), raising the possibility that homotopic coherence may be a universal attribute of healthy brain function.

Any functional differences we observed between the human and macaque datasets could result in part from cross-species differences but might result from differences in fMRI acquisition. The macaque fMRI data were acquired under low-dose anesthesia, and although this method is known to produce robust patterns of FC that are homologous to human FC networks (57), it may affect the temporal structure of FC at higher doses (58). Interhemispheric FC, in particular, is vulnerable to isoflurane in a dose-dependent fashion (59), and this vulnerability may explain why the difference in FC strength between intrahemispheric and heterotopic connections was more pronounced in the macaque than in the human dataset. Future studies using fMRI acquired in awake animals will be needed to investigate cross-species differences in interhemispheric coordination more directly.

Although we found evidence that homotopic connections are more stable across resting-state and IR conditions, it is important to note that this effect may not necessarily generalize to all possible conditions and tasks or to all possible homotopic connections. This caveat is particularly relevant for experimental manipulations that are expected to engage unilateral homotopic region pairs—rather than bilateral homotopic region pairs—directly. For instance, FC between homotopic primary motor regions would be expected to differ depending on whether a participant is engaged in a unimanual or bimanual finger-tapping task. Likewise, FC between homotopic primary visual cortices would be expected to differ depending on whether a visual stimulus is presented in a single hemifield or across the entire visual field.

Summary

Taken together, the present results bring into focus a class of functional connections that appear to have a unique role in large-scale network communication. Despite a perpetually changing landscape of FC, homotopic connections remain stable. This generic cross-species feature of FC is largely supported by the underlying anatomy, which may provide stability in the face of a dynamically changing environment.

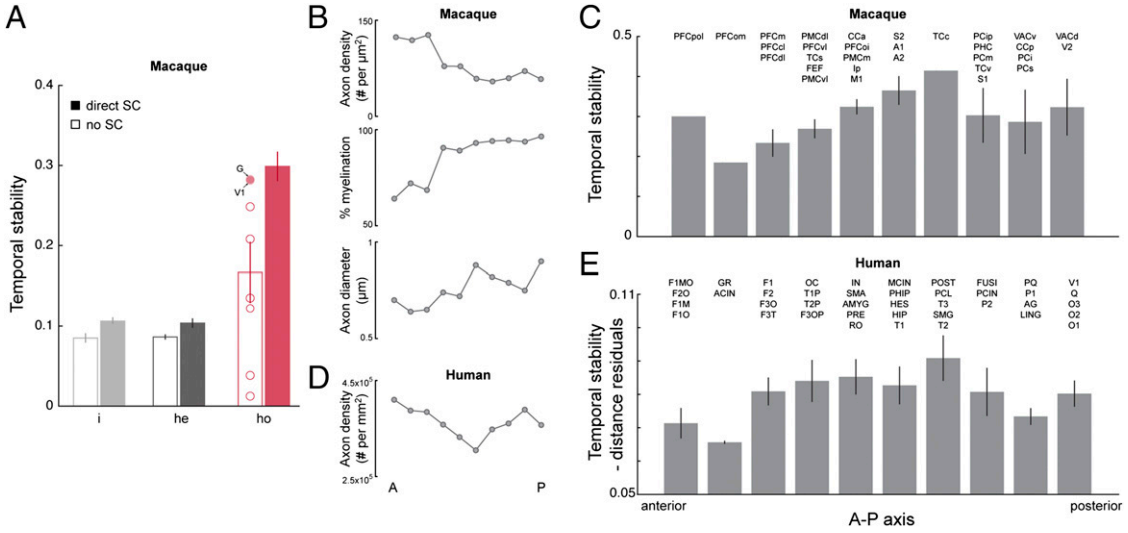

Fig. 4. (*A*) Temporal stability varies as a function of structural connectivity in macaques. Mean (± SEM) FC autocorrelation coefficients for intrahemispheric (i), heterotopic (he), and homotopic (ho) connections. Filled bars show functional connections with direct underlying anatomical connectivity; open bars show functional connections without direct anatomical connectivity. Outlier (greater than mean + 1 SD) homotopic pairs without direct anatomical connectivity are indicated by filled circles; nonoutlier pairs are indicated by open circles. (*B*) The axonal composition of the macaque CC varies along the A–P axis. The figure was produced using data reported in ref. 25. The SE for all values is greater than ± 5%. (*C*) Mean (± SEM) temporal stability of structurally connected homotopic regions varies along the macaque A–P axis. (*D*) Overall axonal density (for fiber diameters >0.4 μm) of the human CC varies along the A–P axis. The figure was produced using data reported in ref. 28 (see *SI Methods*). (*E*) Mean (± SEM) temporal stability of homotopic cortical regions varies along the human A–P axis. Homotopic connections falling within each bin as indicated (see Table S4 for macaque ROI abbreviations and ref. 61 for AAL abbreviations). All temporal stability data were computed using a 60-s window size. See Figs. S4 (macaque) and S5 (human) for other window sizes and fiber diameters.

Methods

Human Dataset. Data acquisition, image preprocessing, and analysis parameters of the human dataset have been described in detail previously (16, 20) and are outlined in *SI Methods*. BOLD-fMRI and behavioral data were collected from 17 (12 female) healthy participants (mean age = 24.2 y; SD = 5.95 y). All participants provided written informed consent as administered by the Institutional Review Board of the University of Michigan. Participants were paid $25/h for their participation.

Macaque Dataset. Animal preparation, data acquisition, image preprocessing, and the anatomical dataset have been described in detail previously (17, 60) and are outlined in *SI Methods*. BOLD-fMRI data were obtained from six (four female) macaque monkeys (*Macaca fascicularis*; mean weight = 4.58 kg; SD = 1.4 kg). All surgical and experimental protocols were approved by the Animal Use Subcommittee of the University of Western Ontario Council on Animal Care and were in accordance with the Canadian Council on Animal Care guidelines.

Data Analysis. Whole-brain fMRI time series were computed for 116 ROIs based on the Automated Anatomical Labeling (AAL) parcellation (61) for the human dataset and 76 ROIs based on the Regional Map parcellation (62) for the macaque dataset. Therefore there were 58 homotopic pairs for the human and 38 homotopic pairs for the macaque dataset. Heterotopic and intrahemispheric connections each numbered 3,306 and 1,406 in the human and macaque datasets, respectively. For the human dataset, ROI time series were computed by taking the mean signal intensity across all voxels. For the macaque dataset, ROI time series were computed using a weighted probabilistic procedure that favored voxels nearer the ROI centroid (60).

Condition Stability. fMRI time series were correlated to form a full correlation matrix for all regions correlated with all other regions for each subject and condition. The upper triangles of these FC matrices were reshaped as vectors and stacked to form a data matrix ordered by subject, then by condition (Fig. 2*A*). For the human dataset, this matrix then was correlated with the participants' self-reported index of negative mood so that the resulting matrix was a set of correlation coefficients that expressed the relationship between FC and behavior. For the macaque dataset, the matrix remained as correlation coefficients that expressed FC. A PLS analysis then was performed on these correlation matrices (*SI Methods*). This analysis results in LVs that each contain (*i*) a set of saliences that describes a spatiotemporal brain pattern, (*ii*) a scalar singular value, and (*iii*) a design contrast between conditions. Thus each LV represents a weighted combination of functional connections that optimally relate to the experimental conditions. For the human dataset, each LV represented a weighted combination or the relationship between FC and mood that was optimally varied by the experimental conditions.

To determine condition stability, we computed the absolute value of the salience of each connection for the given LV. Large saliences indicate that the connections change a lot based on changes in condition. Small saliences indicate that the connections are relatively stable independent of condition.

Temporal Stability. Methods for computing the temporal stability of functional connections have been described previously (14). Briefly, a sliding-window approach was used to determine regionwise Pearson correlations of truncated time series of varying lengths (30, 60, and 120 s). The window was advanced in increments of one time point, and the correlation was recalculated to create an FC time series for each pair of regions (Fig. 3*A*). Each FC time series then was cross-correlated with itself to produce a normalized autocorrelation coefficient. The temporal stability of each functional connection was taken as the average autocorrelation coefficient across all lags. We previously have shown that the choice of window size does not affect this measure of temporal stability (14). For brevity, we present data analyses computed from an intermediate window size (60 s) in the main text and an example each of smaller (30-s) and larger (120-s) window sizes in Figs. S1 and S3–S5 and Tables S1–S3.

To enable comparison between our temporal stability findings and previous reports of regional differences in macaque and human callosal fiber connectivity, we divided the ROIs into 10 bins along the A–P axis following the descriptions provided in refs. 25 and 28. See *SI Methods* for details. ROIs falling within each of the 10 A–P bins are noted in Fig. 4*C* (macaque) and Fig. 4*E* (human). Note that these 10 bins are only estimates of the callosal sectors defined in refs. 25 and 28, and regions subserved by each of the sectors in those papers are unlikely to be an exact match to the ones in the present study.

ACKNOWLEDGMENTS. This work was supported in part by Tom and Kitty Stoner's TKF Foundation grant (to M.G.B.), J. S. McDonnell Foundation Understanding Human Cognition Collaborative Grant 220020255 (to A.R.M.), National Institute of Mental Health Grant MH 60655 (to J.J.), and Canadian Institutes of Health Research (CIHR) Grant MOP 89785 (to S.E.). K.S. held a Fellowship Award from the CIHR.

1. Tononi G, Sporns O, Edelman GM (1994) A measure for brain complexity: Relating functional segregation and integration in the nervous system. *Proc Natl Acad Sci USA* 91(11):5033–5037.
2. Park H-J, Friston K (2013) Structural and functional brain networks: From connections to cognition. *Science* 342(6158):1238411.
3. Jo HJ, Saad ZS, Gotts SJ, Martin A, Cox RW (2012) Quantifying agreement between anatomical and functional interhemispheric correspondences in the resting brain. *PLoS ONE* 7(11):e48847.
4. Salvador R, et al. (2005) Neurophysiological architecture of functional magnetic resonance images of human brain. *Cereb Cortex* 15(9):1332–1342.
5. Hofer S, Frahm J (2006) Topography of the human corpus callosum revisited—comprehensive fiber tractography using diffusion tensor magnetic resonance imaging. *Neuroimage* 32(3):989–994.
6. Aboitiz F (1992) Brain connections: Interhemispheric fiber systems and anatomical brain asymmetries in humans. *Biol Res* 25(2):51–61.
7. Jarbo K, Verstynen T, Schneider W (2012) In vivo quantification of global connectivity in the human corpus callosum. *Neuroimage* 59(3):1988–1996.
8. Lowe MJ, et al. (2008) Resting state sensorimotor functional connectivity in multiple sclerosis inversely correlates with transcallosal motor pathway transverse diffusivity. *Hum Brain Mapp* 29(7):818–827.
9. Quigley M, et al. (2003) Role of the corpus callosum in functional connectivity. *AJNR Am J Neuroradiol* 24(2):208–212.
10. Hutchison RM, et al. (2013) Dynamic functional connectivity: Promise, issues, and interpretations. *Neuroimage* 80:360–378.
11. Deco G, Jirsa VK, McIntosh AR (2011) Emerging concepts for the dynamical organization of resting-state activity in the brain. *Nat Rev Neurosci* 12(1):43–56.
12. Gonzalez-Castillo J, et al. (2014) The spatial structure of resting state connectivity stability on the scale of minutes. *Front Neurosci* 8(June):138.
13. Zalesky A, Fornito A, Cocchi L, Gollo LL, Breakspear M (2014) Time-resolved resting-state brain networks. *Proc Natl Acad Sci USA* 111(28):10341–10346.
14. Shen K, Hutchison RM, Bezgin G, Everling S, McIntosh AR (2015) Network structure shapes spontaneous functional connectivity dynamics. *J Neurosci* 35(14):5579–5588.
15. Hellyer PJ, et al. (2014) The control of global brain dynamics: Opposing actions of frontoparietal control and default mode networks on attention. *J Neurosci* 34(2):451–461.
16. Berman MG, et al. (2014) Does resting-state connectivity reflect depressive rumination? A tale of two analyses. *Neuroimage* 103:267–279.
17. Hutchison RM, et al. (2011) Resting-state networks in the macaque at 7 T. *Neuroimage* 56(3):1546–1555.
18. Stark DE, et al. (2008) Regional variation in interhemispheric coordination of intrinsic hemodynamic fluctuations. *J Neurosci* 28(51):13754–13764.
19. McIntosh AR, Mišić B (2013) Multivariate statistical analyses for neuroimaging data. *Annu Rev Psychol* 64:499–525.
20. Mišić B, et al. (2014) The functional connectivity landscape of the human brain. *PLoS ONE* 9(10):e111007.
21. Stephan KE, et al. (2001) Advanced database methodology for the Collation of Connectivity data on the Macaque brain (CoCoMac). *Philos Trans R Soc Lond B Biol Sci* 356(1412):1159–1186.
22. Bakker R, Wachtler T, Diesmann M (2012) CoCoMac 2.0 and the future of tract-tracing databases. *Front Neuroinform* 6(December):30.
23. Demeter S, Rosene DL, Van Hoesen GW (1985) Interhemispheric pathways of the hippocampal formation, presubiculum, and entorhinal and posterior parahippocampal cortices in the rhesus monkey: The structure and organization of the hippocampal commissures. *J Comp Neurol* 233(1):30–47.
24. Van Essen DC, Newsome WT, Bixby JL (1982) The pattern of interhemispheric connections and its relationship to extrastriate visual areas in the macaque monkey. *J Neurosci* 2(3):265–283.
25. Lamantia AS, Rakic P (1990) Cytological and quantitative characteristics of four cerebral commissures in the rhesus monkey. *J Comp Neurol* 291(4):520–537.
26. LaMantia AS, Rakic P (1990) Axon overproduction and elimination in the corpus callosum of the developing rhesus monkey. *J Neurosci* 10(7):2156–2175.
27. Caminiti R, Ghaziri H, Galuske R, Hof PR, Innocenti GM (2009) Evolution amplified processing with temporally dispersed slow neuronal connectivity in primates. *Proc Natl Acad Sci USA* 106(46):19551–19556.
28. Aboitiz F, Scheibel AB, Fisher RS, Zaidel E (1992) Fiber composition of the human corpus callosum. *Brain Res* 598(1-2):143–153.
29. O'Reilly JX, et al. (2013) Causal effect of disconnection lesions on interhemispheric functional connectivity in rhesus monkeys. *Proc Natl Acad Sci USA* 110(34):13982–13987.
30. Johnston JM, et al. (2008) Loss of resting interhemispheric functional connectivity after complete section of the corpus callosum. *J Neurosci* 28(25):6453–6458.
31. Glickstein M, Berlucchi G (2008) Classical disconnection studies of the corpus callosum. *Cortex* 44(8):914–927.
32. Tyszka JM, Kennedy DP, Adolphs R, Paul LK (2011) Intact bilateral resting-state networks in the absence of the corpus callosum. *J Neurosci* 31(42):15154–15162.
33. Vincent JL, et al. (2007) Intrinsic functional architecture in the anaesthetized monkey brain. *Nature* 447(7140):83–86.
34. Tovar-Moll F, et al. (2014) Structural and functional brain rewiring clarifies preserved interhemispheric transfer in humans born without the corpus callosum. *Proc Natl Acad Sci USA* 111(21):7843–7848.
35. Honey CJ, et al. (2009) Predicting human resting-state functional connectivity from structural connectivity. *Proc Natl Acad Sci USA* 106(6):2035–2040.
36. Markov NT, et al. (2013) Cortical high-density counterstream architectures. *Science* 342(6158):1238406.
37. Putnam MC, Wig GS, Grafton ST, Kelley WM, Gazzaniga MS (2008) Structural organization of the corpus callosum predicts the extent and impact of cortical activity in the nondominant hemisphere. *J Neurosci* 28(11):2912–2918.
38. Aboitiz F, Montiel J (2003) One hundred million years of interhemispheric communication: The history of the corpus callosum. *Braz J Med Biol Res* 36(4):409–420.
39. Wang SS-H, et al. (2008) Functional trade-offs in white matter axonal scaling. *J Neurosci* 28(15):4047–4056.
40. Kennedy H, Dehay C (1988) Functional implications of the anatomical organization of the callosal projections of visual areas V1 and V2 in the macaque monkey. *Behav Brain Res* 29(3):225–236.
41. Tootell RB, et al. (1998) The retinotopy of visual spatial attention. *Neuron* 21(6):1409–1422.
42. Saenz M, Fine I (2010) Topographic organization of V1 projections through the corpus callosum in humans. *Neuroimage* 52(4):1224–1229.
43. Knyazeva MG (2013) Splenium of corpus callosum: Patterns of interhemispheric interaction in children and adults. *Neural Plast* 2013:639430.
44. Van Essen DC (2005) Corticocortical and thalamocortical information flow in the primate visual system. *Prog Brain Res* 149(4):173–185.
45. Everitt BJ, Robbins TW (1997) Central cholinergic systems and cognition. *Annu Rev Psychol* 48:649–684.
46. Turchi J, et al. (2014) Transient inactivation of basal forebrain subregions shapes spontaneous fMRI correlations in the macaque. Program No. 481.05. *Neuroscience 2014 Abstracts* (Society for Neuroscience Washington, DC). Available at bit.ly/1yQ4pde. Accessed April 22, 2015.
47. Cossell L, et al. (2015) Functional organization of excitatory synaptic strength in primary visual cortex. *Nature* 518(7539):399–403.
48. Sherman SM, Guillery RW (1998) On the actions that one nerve cell can have on another: Distinguishing "drivers" from "modulators". *Proc Natl Acad Sci USA* 95(12):7121–7126.
49. Deco G, et al. (2014) Identification of optimal structural connectivity using functional connectivity and neural modeling. *J Neurosci* 34(23):7910–7916.
50. Messé A, Rudrauf D, Benali H, Marrelec G (2014) Relating structure and function in the human brain: Relative contributions of anatomy, stationary dynamics, and nonstationarities. *PLOS Comput Biol* 10(3):e1003530.
51. Rilling JK, Insel TR (1999) Differential expansion of neural projection systems in primate brain evolution. *Neuroreport* 10(7):1453–1459.
52. Hopkins WD, Rilling JK (2000) A comparative MRI study of the relationship between neuroanatomical asymmetry and interhemispheric connectivity in primates: Implication for the evolution of functional asymmetries. *Behav Neurosci* 114(4):739–748.
53. Ringo JL, Doty RW, Demeter S, Simard PY (1994) Time is of the essence: A conjecture that hemispheric specialization arises from interhemispheric conduction delay. *Cereb Cortex* 4(4):331–343.
54. Cipollini B, Cottrell G (2014) Interhemispheric functional connectivity is not selectively reduced in larger-brained species. Program No. 446.03. *Neuroscience 2014 Abstracts* (Society for Neuroscience, Washington, DC). Available at bit.ly/1bjd8Kn. Accessed April 22, 2015.
55. Olivares R, Michalland S, Aboitiz F (2000) Cross-species and intraspecies morphometric analysis of the corpus callosum. *Brain Behav Evol* 55(1):37–43.
56. Zhang J, Kendrick KM, Lu G, Feng J (2014) The fault lies on the other side: Altered brain functional connectivity in psychiatric disorders is mainly caused by counterpart regions in the opposite hemisphere. *Cereb Cortex*, 10.1093/cercor/bhu.
57. Hutchison RM, Everling S (2012) Monkey in the middle: Why non-human primates are needed to bridge the gap in resting-state investigations. *Front Neuroanat* 6(July):29.
58. Barttfeld P, et al. (2015) Signature of consciousness in the dynamics of resting-state brain activity. *Proc Natl Acad Sci USA* 112(3):887–892.
59. Hutchison RM, Hutchison M, Manning KY, Menon RS, Everling S (2014) Isoflurane induces dose-dependent alterations in the cortical connectivity profiles and dynamic properties of the brain's functional architecture. *Hum Brain Mapp* 35(12):5754–5775.
60. Shen K, et al. (2012) Information processing architecture of functionally defined clusters in the macaque cortex. *J Neurosci* 32(48):17465–17476.
61. Tzourio-Mazoyer N, et al. (2002) Automated anatomical labeling of activations in SPM using a macroscopic anatomical parcellation of the MNI MRI single-subject brain. *Neuroimage* 15(1):273–289.
62. Kötter R, Wanke E (2005) Mapping brains without coordinates. *Philos Trans R Soc Lond B Biol Sci* 360(1456):751–766.